

High-mass K^* production in K^+d interactions at $9 \text{ GeV}/c$ [†]

D. D. Carmony, H. W. Clopp,[‡] A. F. Garfinkel, and L. K. Rangan
Purdue University, West Lafayette, Indiana 47907

R. L. Lander, D. E. Pellett, and P. M. Yager
University of California at Davis, Davis, California 95616

F. T. Meiere and W. L. Yen
Indiana University-Purdue University at Indianapolis, Indianapolis, Indiana 46205
(Received 21 March 1977)

We have observed $K^*(1760)$ and $K^*(2100)$ production in a $10\text{-event}/\mu\text{b}$ K^+d experiment at $9 \text{ GeV}/c$. The $K^*(1760)$ has a mass of $1769 \pm 12 \text{ MeV}$ and a width of $132 \pm 50 \text{ MeV}$ and the $K^*(2100)$ has a mass of $2115 \pm 46 \text{ MeV}$ and a width of $300 \pm 200 \text{ MeV}$. Branching ratios for decay into various final states are presented and evidence for decay into two, three, and four scalar mesons is presented. The spin-parity of the $K^*(1760)$ is found to be 3^- . The $K^*(2100)$ is compatible with a 4^+ assignment.

I. INTRODUCTION

In previous articles we reported the discovery¹ of the $K^*(1760)$ meson which has $K\pi$, $K\rho$, and $K^*(890)\pi$ decay modes and which is a member of the $J^P = 3^-$ nonet.² We also reported evidence for an additional state² which we denote $K^*(2100)$. We report here on a further study of the above decay modes for these mesons and present evidence for other decay modes.

The current experiment was carried out in an rf-separated K^+ beam of momentum $9.04 \text{ GeV}/c$ in the BNL 80-in. deuterium-filled bubble chamber. A total of 400 000 pictures were taken and analyzed. The charge-exchange reactions previously studied in Ref. 1 are reported on here with an increase in data of 30 and 200%, respectively, that is,³

$$K^+n \rightarrow pK^+\pi^- \quad 4581 \text{ events}, \quad \sigma = 505 \pm 20 \mu\text{b} \quad (1)$$

and

$$K^+n \rightarrow pK^0\pi^+\pi^- \quad 1540 \text{ events}, \quad \sigma = 205 \pm 15 \mu\text{b}. \quad (2)$$

Here we have also studied the additional charge-exchange reactions

$$K^+n \rightarrow pK^+\pi^-\pi^0 \quad 1984 \text{ events}, \quad \sigma = 275 \pm 35 \mu\text{b}, \quad (3)$$

$$K^+n \rightarrow pK^+\pi^+\pi^-\pi^- \quad 1310 \text{ events}, \quad \sigma = 167 \pm 20 \mu\text{b}, \quad (4)$$

$$K^+n \rightarrow pK^0\pi^+\pi^-\pi^0 \quad 710 \text{ events}, \quad \sigma = 275 \pm 30 \mu\text{b}, \quad (5)$$

and

$$K^+n \rightarrow pK^+\pi^+\pi^-\pi^0 \quad 1461 \text{ events}, \quad \sigma = 200 \pm 45 \mu\text{b}. \quad (6)$$

The events were measured on the Purdue SMP's (image-plane scanning and measuring projectors) with on-line geometry (TVGP). Subsequently, kinematic fitting was carried out using the program SQUAW. Those events determined to be candidates for the charge-exchange reactions with only one constraint, that is, about two-thirds of the events of reaction (2) and all the events of reactions (3), (5), and (6), were then examined for ionization information by a physicist and remeasured on precision film-plane devices. The mass resolution in the region of interest is about 12 MeV for the reactions with no missing neutrals and 30–60 MeV for the others, depending on whether the spectator is visible or not. In the various reactions we have always required $|t'| < 1.0 (\text{GeV}/c)^2$, where $t' = t - t_{\text{min}}$ and where t is the four-momentum transfer squared between the incident K^+ and the outgoing meson system. This cut allows the proton to be identified unambiguously by ionization. We also require that the one-constraint reactions fit with a χ^2 probability of at least 5%. The four-constraint hypotheses are accepted with a χ^2 probability of 0.1% or greater. Finally, for hypotheses with a visible spectator we require^{3,4} that the spectator have a momentum of less than 300 MeV/c.

II. THE $K\pi$ MASS SPECTRUM

With the above-discussed cuts we obtain 4581 events of the four-constraint reaction (1). The dominant features of the $p\pi^-K^+$ Dalitz plot (Fig. 1) are a low-mass $p\pi^-$ enhancement which has been previously reported on^{5,6} and a number of enhancements in the $K\pi$ mass spectrum. An analysis of the $K^*(890)$ as well as evidence for an S-wave $K\pi$ state just below the $K^*(1420)$ have been presented elsewhere.^{7,8} In the present work we shall discuss

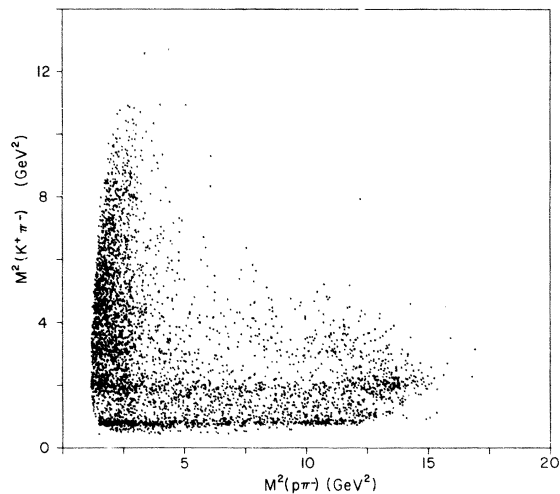


FIG. 1. Dalitz plot $M^2(p\pi^-)$ vs $M^2(K^+\pi^-)$ for reaction (1).

the evidence for strange mesons of mass greater than that of the $K^*(1420)$. The most prominent feature of the $K\pi$ mass spectrum above the $K^*(1420)$ is, as seen in Fig. 2, a sharp rise at a mass of about 1.65 GeV. The events between 1.65 and 2.2

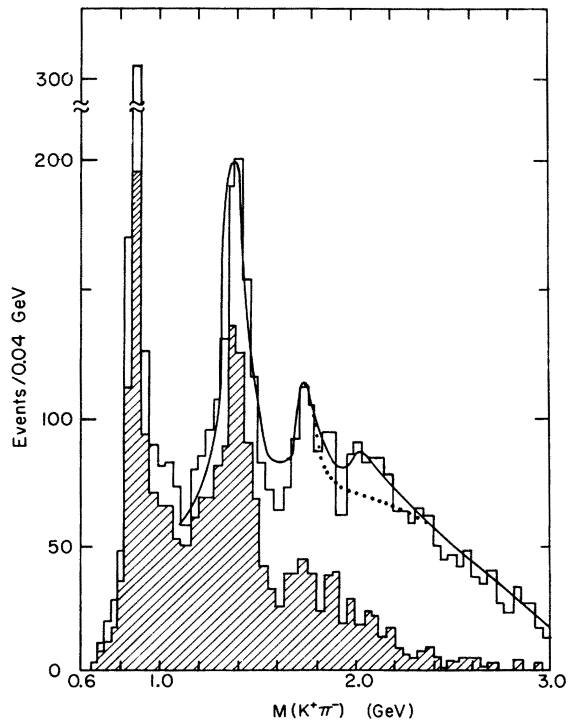


FIG. 2. The $K^+\pi^-$ effective mass distribution in the $pK^+\pi^-$ final state. The shaded histogram is for events with $M(p\pi^-) > 1.7$ GeV. The solid curve is a fit to the histogram with background and three simple Breit-Wigner resonances. The dotted curve is the best fit with only two Breit-Wigner resonances (see Table I).

GeV are produced with a momentum transfer between the incident K^* and the outgoing meson system which is nearly mass independent and approximately of the form $e^{-8|t|}$.

If the $K\pi$ mass interval 1.0 to 3.0 GeV [with a small $K^*(890)$ tail removed] is fitted using the method of least squares to a quadratic background (three parameters) plus a $K^*(1420)$ Breit-Wigner resonance and one additional Breit-Wigner resonance (simple Breit-Wigner resonances are used), a barely acceptable fit (χ^2 probability 1%) is found. The inclusion of a second high-mass resonance gives a very good fit to the data as seen in Table I and Fig. 2 and improves the χ^2 probability of the fit to 37%

Additional evidence from reaction (1) alone that there are two structures in the high-mass region is the observation (Fig. 2, shaded histogram) that the lower half of the enhancement is produced for $M_{p\pi} > 1.7$ GeV, whereas the upper half is produced primarily in association with the $p\pi^-$ low-mass enhancement.

Finally in Fig. 3 we show the unnormalized Y_6^0 and Y_8^0 moments for all events with $|t'| < 0.2$

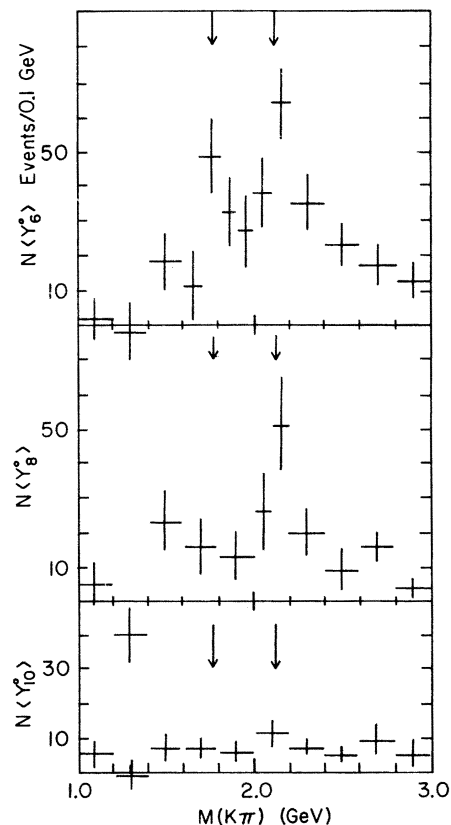


FIG. 3. The unnormalized Y_6^0 , Y_8^0 , and Y_{10}^0 moments as a function of $K^+\pi^-$ mass for all the events of reaction (1) with $-t' < 0.02$ GeV $^2/c^2$ (Gottfried-Jackson frame).

TABLE I. Fits to $K^0\pi^+\pi^-$ and/or $K^+\pi^-$ mass spectrum. Masses and widths are in MeV. Amounts are events above background.

Fits to two resonances and quadratic background				
Quantity	$K\pi$	$K^0\pi^+\pi^-$	Both	
Mass	1404 ± 10	1428 ± 22	1406 ± 10	
Width	107 ± 18	238 ± 90	135 ± 10	
Amount $K\pi\pi$...	387 ± 60	266 ± 35	
Amount $K\pi$	573 ± 50	...	644 ± 20	
Mass	1758 ± 12	1789 ± 18	1780 ± 5	
Width	55 ± 62	85 ± 50	112 ± 10	
Amount $K\pi\pi$...	127 ± 30	150 ± 15	
Amount $K\pi$	95 ± 25	...	125 ± 45	
Probability of fit	1%	11%	0.05%	
Fits to three resonances and quadratic background				
Quantity	$K\pi$	$K^0\pi^+\pi^-$	Both	Scale factor
Mass	1404 ± 10	1424 ± 20	1406 ± 9	0.9
Width	129 ± 35	237 ± 50	144 ± 30	1.9
Amount $K\pi\pi$...	404 ± 30	299 ± 30	
Amount $K\pi$	716 ± 90	...	739 ± 40	
Mass	1756 ± 15	1785 ± 20	1769 ± 12	1.2
Width	77 ± 60	125 ± 40	132 ± 50	0.9
Amount $K\pi\pi$...	172 ± 30	180 ± 35	
Amount $K\pi$	142 ± 20	...	200 ± 41	
Mass	2094 ± 65	2146 ± 30	2115 ± 46	1.1
Width	540 ± 300	52 ± 50	300 ± 200	5.1
Amount $K\pi\pi$...	64 ± 25	115 ± 50	
Amount $K\pi$	673 ± 200	...	373 ± 50	
Probability of fit	37%	67%	10%	

(GeV/c)². The behavior of these moments is seen to be different in the lower and upper portions of the enhancement, in particular the Y_8^0 moment becomes sizable only in the higher mass structure.

III. THE $K\pi\pi$ FINAL STATES

We turn now to a discussion of reaction (2), namely in the $pK^0\pi^+\pi^-$ final state and reaction (3), the $pK^+\pi^-\pi^0$ final state. These two reactions are initially ambiguous in about 25% of the cases in the sense that both fits have at least a 5% probability of fit and the K^+/π^+ ambiguity cannot be resolved by ionization. Examination of the single-particle spectra of the unambiguous events of reaction (2) where the K^0 is visible shows that we can require that the laboratory momentum of the K^0 be greater than 1.5 GeV/c and that the momentum of the π^+ be less than 7.0 GeV/c in reaction (2). Resolving the remaining ambiguities on the basis of χ^2 probability results in a clean sample of reaction (2) as determined by the observation that the $\pi^+\pi^-$ mass spectrum when interpreted as a $K^+\pi^-$ mass spectrum no longer shows any $K^*(890)$ signal. Reaction (3) remains rather contaminated perhaps by multiple-

π^0 events, and appears to be of rather poorer resolution. In addition, it is not as useful for the study of $K\pi\pi$ states because $\Delta(1236)K^*(890)$ production is strong.

In Fig. 4 we show the (a) $p\pi^-$, (b) $K^0\pi^+$, and (c) $\pi^+\pi^-$ mass spectra of reaction (2). The events which are $\Delta^0(1236)$, $K^*(890)$ are shown shaded.⁹ Removal of these events very nearly removes the Δ^0 signal. The $K\pi$ and $\pi\pi$ mass spectra show considerable $K^*(890)$ and ρ production. Figure 5 shows the (a) $p\pi^-$, (b) $p\pi^0$, (c) $K^+\pi^-$, (d) $K^+\pi^0$, and (e) $\pi^-\pi^0$ mass spectra for reaction (3). Again Δ^0 production is primarily in association with the $K^*(890)$ (shaded events). The production of the $K^*(890)$ and the ρ meson are less prominent because there are two ways of making the $K^*(890)$ and because the resolution is poorer. In the subsequent analysis the $\Delta(1236)K^*(890)$ events have been removed leaving 1441 and 1734 events in reactions (2) and (3), respectively. In Fig. 6(a) the $K^0\pi^+\pi^-$ effective mass spectrum is shown and in Fig. 6(b) the $K^+\pi^-\pi^0$ mass spectrum is presented. The $K^0\pi^+\pi^-$ mass spectrum has been fitted with a quadratic background plus two or three Breit-

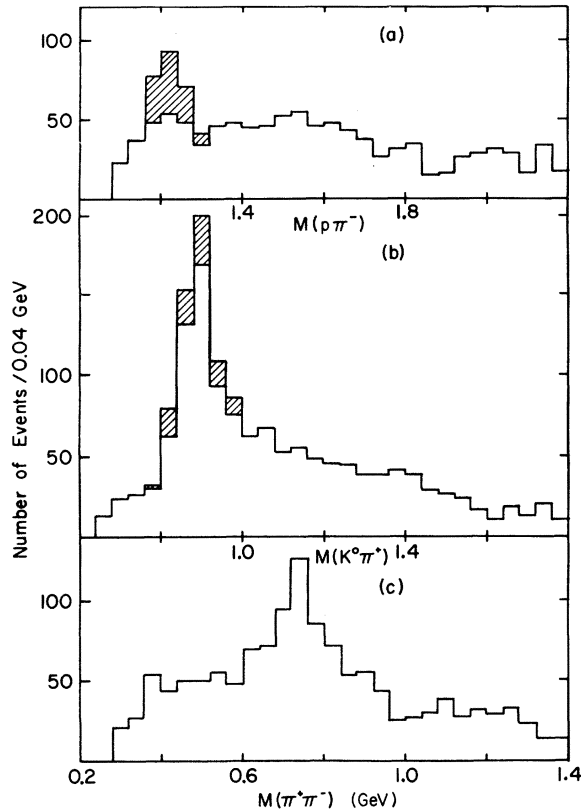


FIG. 4. Two-body effective mass distributions in the final state $pK^0\pi^+\pi^-$. (a) $M(p\pi^-)$, (b) $M(K^0\pi^+)$, (c) $M(K^+\pi^0)$. The events shown shaded are $K^*(890)$, $\Delta^0(1236)$ events which have been removed from (c).

Wigner resonances whose parameters are given in Table I. An acceptable fit (11%) can be obtained without the third resonance but then the 2100-MeV region shows a four-standard-deviation excess. Inclusion of the third Breit-Wigner resonance increases the goodness of fit to 67%. The two enhancements are not resolved in the $K^*\pi^-\pi^0$ final state. If, however, a $K^*(890)^0$, which is the only important two-body state seen in Fig. 5, is required, then the $K^*\pi^0$ effective mass distribution [Fig. 6(b), shaded] shows a small $K^*(1760)$ signal compatible with isospin requirements.

If the $K\pi$ and $K^0\pi^+\pi^-$ enhancements are assumed to be different decay modes of the same resonances and if only one resonance is assumed in addition to the $K^*(1420)$, then the $K^*\pi^-$ and $K^0\pi^+\pi^-$ mass spectra are clearly incompatible (χ^2 probability = 0.05%). If, however, we assume separate quadratic backgrounds and resonant amounts for reactions (1) and (2) but require the same mass and width for the three simple Breit-Wigner resonances, we obtain as seen in Fig. 7 a reasonable fit to the data for masses in the 1- to 3-GeV/ c region (10% probabil-

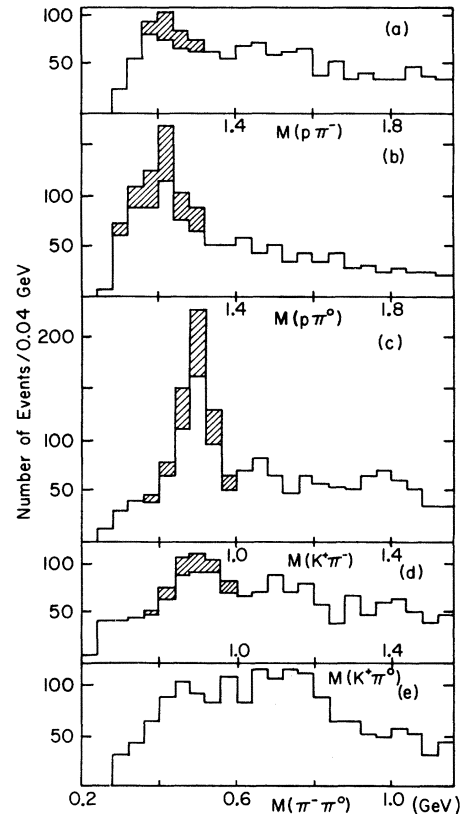


FIG. 5. Two-body effective mass distributions in the final state $pK^+\pi^-\pi^0$. (a) $M(p\pi^-)$, (b) $M(p\pi^0)$, (c) $M(K^+\pi^-)$, (d) $M(K^+\pi^0)$, (e) $M(\pi^-\pi^0)$. The events shown shaded are $K^*(890)^+$, $\Delta(1236)^0$ events in (a) and (d) and $K^*(890)^0$, $\Delta(1236)^+$ events in (b) and (c). The $K^*\Delta$ events are removed from (e).

ity) with the parameters given in Table I. Furthermore, we show in Table I the scale factor associated with each of these parameters, where S , the scale factor,¹⁰ is a measure of the internal compatibility of the parameters when determined separately in the two- and three-body final states. We see that only the width of the third state is internally inconsistent. We have doubled the error on the overall fit to the width of the $K^*(2100)$ because of this statistical problem.

IV. ADDITIONAL EVIDENCE FOR HIGH-MASS STATES AND BRANCHING RATIOS

We turn now to a study of decay modes of the $K^*(1760)$ and $K^*(2100)$ which result in final states with four pseudoscalar mesons. We have examined the final state (4), namely $pK^+\pi^+\pi^-\pi^-$, and the final state (5), namely $pK^0\pi^+\pi^-\pi^0$. Reaction (4) is a four-constraint fit and if the spectator proton is seen ($\frac{1}{3}$ of the time) the K^*/π^+ ambiguity is resolved

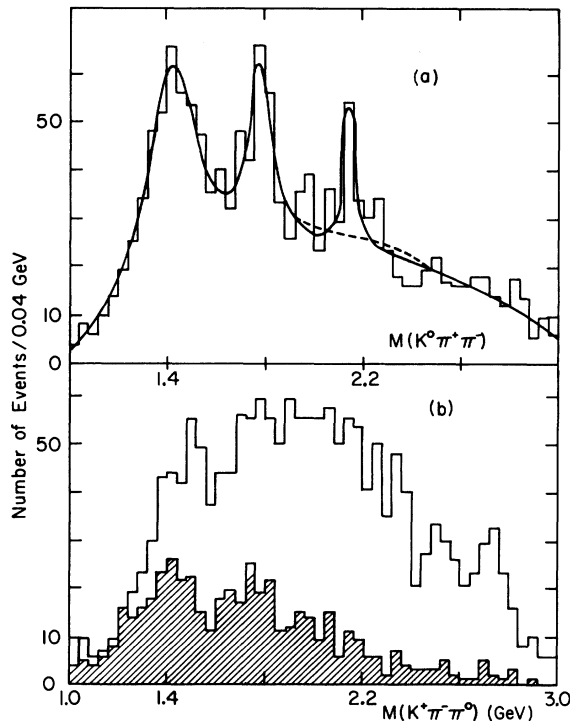


FIG. 6. (a) $K^0\pi^+\pi^-$ effective mass distribution from reaction (2). The solid curve is a fit to the histogram with background and three Breit-Wigner resonances. The dashed curve is with two Breit-Wigner resonances. (b) $K^+\pi^-\pi^0$ effective mass distribution from reaction (3). The events which are $K^*(890)\pi^0$ are shown shaded.

uniquely by the kinematics program. When the spectator is not seen, about 15% of the events are wrongly chosen if the K^+/π^+ ambiguity is resolved on the basis of χ^2 . The amount of contamination is measured by looking for a $K^*(890)$ in the "wrong" track combination. We are, however, primarily interested in the $K^*(890)\rho$ mass spectrum. Since examination of the unique events with visible spectators shows that the probability of an event being a " $K^*\rho$ event" with the wrong K^+/π^+ assignment is entirely negligible, we can still obtain a pure sample of $K^*\rho$ events. The candidates for reaction (5) come from SMP measurements of all the three- and four-prong plus vee events. Those compatible with the π^0 interpretation were remeasured on precision microscopes and appear to be free of contamination.

The $K^+\pi^-$ and $\pi^+\pi^-$ effective mass distributions with two combinations per event are shown in Fig. 8 for reaction (4), and in Fig. 9 the various $K\pi$ and $\pi\pi$ effective masses are shown for reaction (5). These reactions are dominated by $K^*(890)$ production. There is some ρ production, especially in association with $K^*(890)$ production (shown shaded). There is also a small amount (not shown) of

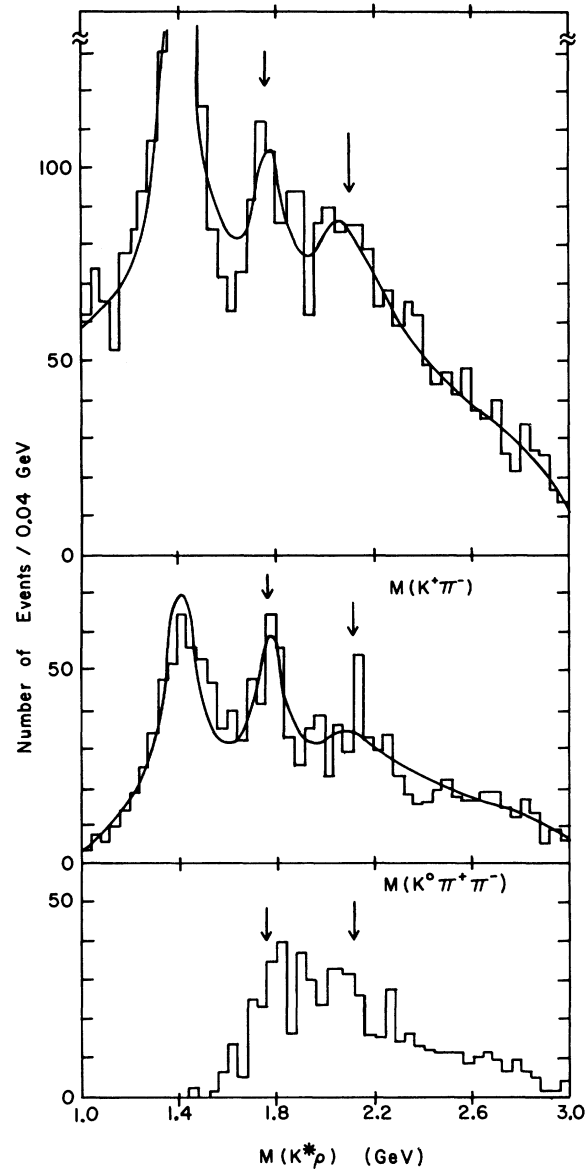


FIG. 7. Upper: $K^+\pi^-$ effective mass distribution from reaction (1) with a small $K^*(890)$ tail removed. Middle: $K^0\pi^+\pi^-$ effective mass distribution from reaction (2). The solid curve is a simultaneous fit to the two histograms with the parameters of Table I. Lower: The $K^*(890)\rho$ effective mass distribution from reactions (4) and (5).

$\Delta^0(1236)$ production in these reactions which we have not removed. The $K^+\pi^-\pi^-\pi^-$ and $K^0\pi^+\pi^-\pi^0$ mass spectra are shown in Fig. 10 with the $K^*(890)\rho$ events shown shaded. The combined $K^*\rho$ mass spectrum is compared to the $K\pi$ and $K\pi\pi$ spectra in Fig. 7. The dominant feature of the $K^*\rho$ mass distribution is an enhancement from 1.68–2.2 GeV. We cannot rule out a single broad enhancement ($\Gamma \sim 500$ MeV), but the most reasonable interpreta-

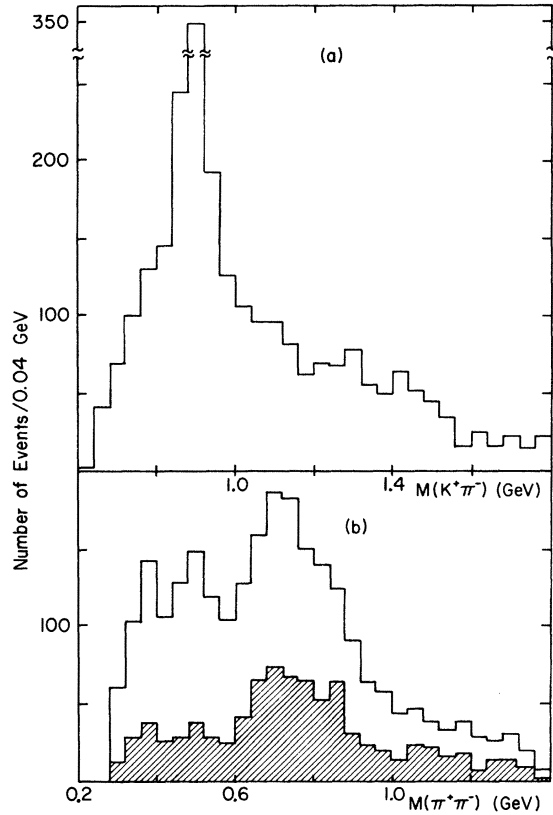


FIG. 8. Effective mass distributions for the final state $pK^+\pi^+\pi^-\pi^-$. (a) $M(K^+\pi^-)$ with two combinations per event. (b) $M(\pi^+\pi^-)$ with two combinations per events. The shaded histogram is the $\pi^+\pi^-$ effective mass distribution when the other $K^+\pi^-$ combination is in the $K^*(890)$ mass interval.

tion is that both the $K^*(1760)$ and $K^*(2100)$ decay into two vector mesons. In addition, in reaction (5) about 40 ω^0 are produced on a background of about 30 events (fig. 11), and these events yield at most 10 $K^*(1760) \rightarrow K\omega$ events. After background corrections are made, no significant statement about the branching into $K\omega$ can be made. Chung *et al.*¹¹ have also reported evidence for a $K\omega$ state which could be associated with the $K^*(1760)$. We see no evidence for $K^*(2100)$ branching into $K\omega$.

In reaction (6) we have examined the final state $pK^+\pi^+\pi^-\pi^0$ for evidence of high-mass K^* production. Here the proton is identified by ionization, but the K^+/π^+ ambiguity is unresolved and each event is plotted twice. In addition, the presence of two π^- mesons leads to further combinatorial background. The only significant two-body final state [Fig. 12(a)] is the $K^*(890)$. In Fig. 12(b) the $\pi^+\pi^-\pi^0$ effective mass is presented and a small ω signal is seen. The $K^+\pi^+\pi^-\pi^0$ effective mass distribution [Fig. 13(a)] shows no structure. If, however, we demand that the event have a $\pi^+\pi^-\pi^0$ mass

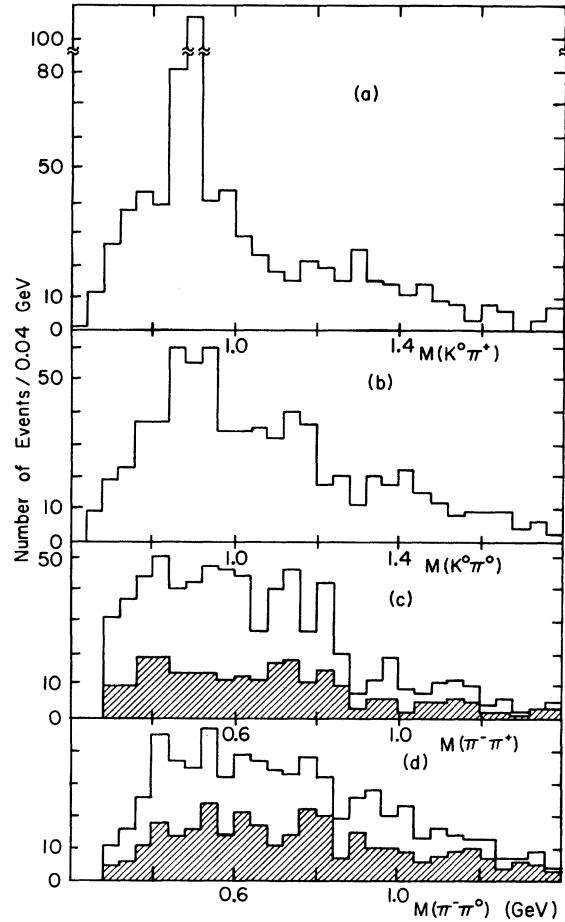


FIG. 9. Effective mass distributions for the final state $pK^0\pi^+\pi^-\pi^0$. (a) $M(K^0\pi^+)$, (b) $M(K^0\pi^0)$, (c) $M(\pi^+\pi^-)$, and (d) $M(\pi^-\pi^0)$. The shaded histograms require the other $K\pi$ combination to be in the $K^*(890)$ mass interval.

in the ω band and that the other two particles form a $K^*(890)$, the resulting mass plot [Fig. 13(b)] is consistent with a small amount of $K^*(1760) \rightarrow K^*(890)\omega$. The peak if it represents $K^*(1760)$ is somewhat mass shifted due to the small Q value of

TABLE II. Branching ratios.

Quantity	$K^*(1760)$	$K^*(2100)$
$K^*(890)\pi/K\pi$	0.54 ± 0.24	0.17 ± 0.07
$K\rho/K\pi$	1.05 ± 0.42	0.16 ± 0.06
$K^*(1420)\pi/K\pi$	< 0.06	0.45 ± 0.18
$Kf/K\pi$	< 0.07	0.05 ± 0.02
$K\omega/K\pi$	0.12 ± 0.10	< 0.1
$K^*(890)\rho/K\pi$	0.60 ± 0.22	0.18 ± 0.10
$K^*(890)\omega/K\pi$	0.04 ± 0.03	< 0.05
$\bar{\Lambda}N/K\pi$...	Seen (?)
$K\pi/\text{all}$	0.28 ± 0.07	0.45 ± 0.2

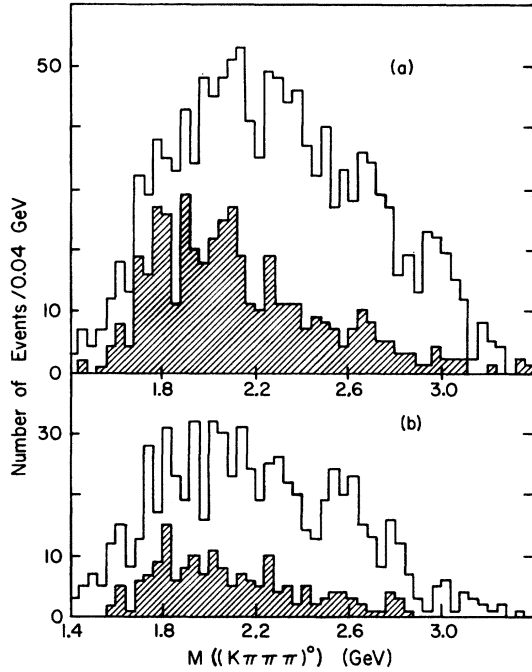


FIG. 10. (a) $K^*\pi^+\pi^-\pi^0$ effective mass distribution from reaction (4). (b) $K^0\pi^+\pi^-\pi^0$ effective mass distribution from reaction (5). Shaded events are $K^*\rho$ events.

the $K^*\omega$ decay mode. No evidence for a $K^*(2100)$ decay into $K^*(890)$ and ω is seen.

The various measured branching ratios (corrected for unseen decays) are tabulated in Table II. The $K^*\pi$ and $K\rho$ amounts were determined as follows: We restrict ourselves to those events of reaction (2) where either the K^0 is visible, or, if it is not visible, we require that the spectator proton be visible, since the remaining events have considerably poorer resolution. We have used a maximum likelihood method to fit the Dalitz plot

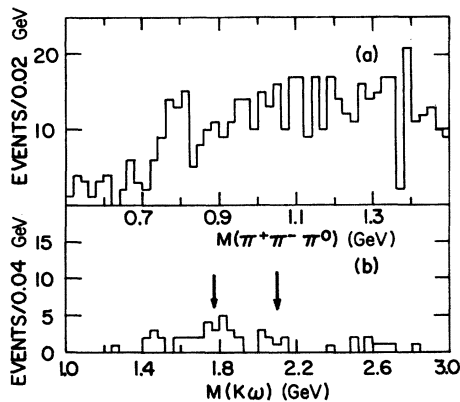


FIG. 11. (a) The $\pi^+\pi^-\pi^0$ effective mass distribution for the $pK^0\pi^+\pi^-\pi^0$ final state. (b) The $K\omega$ effective mass distribution.

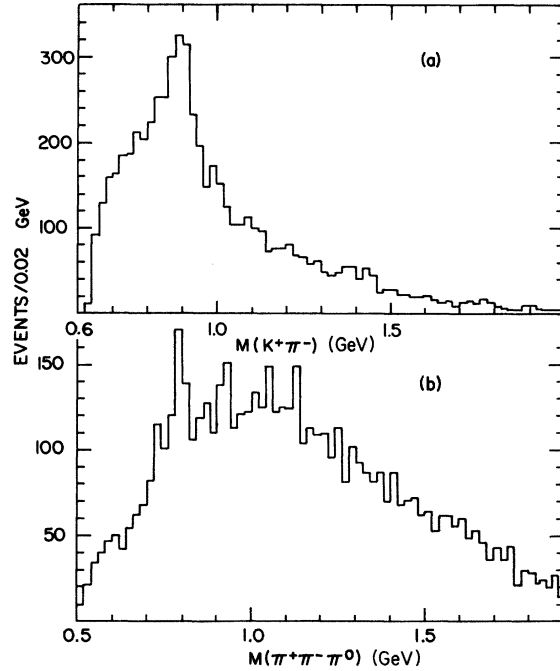


FIG. 12. (a) The $K^*\pi^-$ effective mass distribution for the final state $pK^+\pi^+\pi^-\pi^-\pi^0$ (four combinations per event since K^*/π^+ are ambiguous). (b) The $\pi^+\pi^-\pi^0$ effective mass distribution (four combinations).

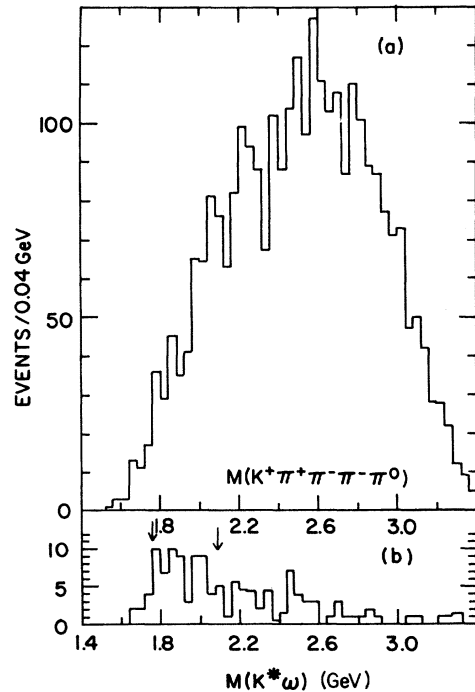


FIG. 13. (a) The $K^*\pi^+\pi^-\pi^0$ effective mass distribution for the $pK^+\pi^+\pi^-\pi^-\pi^0$ final states. (b) The $K^*\pi^+\pi^-\pi^0$ effective mass distribution for events consistent with $K^*\omega$ production.

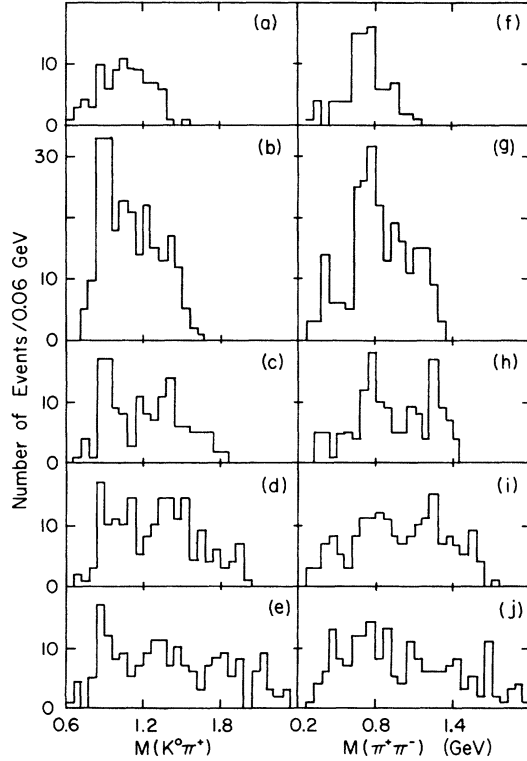


FIG. 14. Various two-body effective masses from the $pK^0\pi^+\pi^-$ final state for the $K\pi\pi$ mass intervals (top to bottom) 1.57–1.67, 1.67–1.87, 1.87–2.05, 2.05–2.25, and 2.25–2.65 GeV. (a)–(e) $K\pi$ effective masses, (f)–(j) $\pi\pi$ effective masses.

for the two high-mass states. After background subtraction we find for the $K^*(1760)$ that the amount of $K^*\pi$ is $33 \pm 12\%$, the amount of $K\rho$ is $48 \pm 14\%$, and the amount of uncorrelated $K\pi\pi$ is $19 \pm 15\%$. For the $K^*(2100)$ the amount of $K^*\pi$ is $51 \pm 15\%$, the amount of $K\rho$ is $49 \pm 15\%$, and the amount of uncorrelated $K\pi\pi$ is $0 \pm 15\%$. Our current value of the $K^*(1760)$ branching ratio $\Gamma(K^*\pi + K\rho)/\Gamma(K\pi)$ is 1.59 ± 0.44 . This is lower than our value in Ref. 1 (2.5 ± 0.6), but as we noted there the amount of $K\pi$ was a lower limit since we then assumed no structure above the $K^*(1760)$. Aguilar-Benitez *et al.*¹²

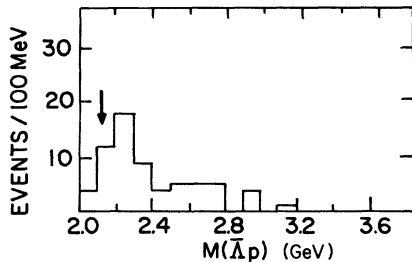


FIG. 15. The $\bar{\Lambda}p$ effective mass distribution for events with an identified $\bar{\Lambda}$.

have reported 0.8 ± 0.4 for this same quantity and Spiro *et al.*¹³ found 0.4 ± 0.60 . Within statistics, all of these are compatible with their weighted average of 1.0 ± 0.3 .

In Fig. 14 we show for reaction (2) the $K^0\pi^+$ (at left) and the $\pi^+\pi^-$ (at right) mass spectra for five intervals of $K^0\pi^+\pi^-$ mass. The mass intervals are (from top to bottom) below the $K^*(1760)$, i.e., 1.57–1.67 GeV, the $K^*(1760)$ region, i.e., 1.67–1.87 GeV, between the two resonances, i.e., 1.87–2.05 GeV, the $K^*(2100)$ region, i.e., 2.05–2.25 GeV, and above the resonances, i.e., 2.25–2.65 GeV. The interval between the two resonances is unfortunately dominated by the resonant tails. The $K^*(2100)$, Fig. 14(d) and 14(i), appears to have $K^*(1420)\pi$ and Kf decay modes as well as $K^*\pi$ and $K\rho$.

We have also examined the $\bar{\Lambda}p$ effective mass of 67 events containing a visible $\bar{\Lambda}$. We select the proton which gives the lowest momentum transfer between the incident K^+ and the outgoing $\bar{\Lambda}p$. In Fig. 15 the $\bar{\Lambda}p$ effective mass is shown and a small peak at ~ 2.2 GeV is evident. If this peak (which could be slightly mass shifted by threshold effects) is associated with the $K^*(2100)$, then this state is the one first reported by Lissauer *et al.*¹⁴

V. SPIN AND PARITY

The absence of high-mass resonances in the reaction¹⁵ $K^-n \rightarrow K^-\pi^+p$ proves that the $K^*(1760)$ and $K^*(2100)$ are isospin- $\frac{1}{2}$ states. The existence of both two- and three-body decay modes restricts the spin and parity J^P to $1^-, 2^+, 3^-, 4^+, \dots$. In Fig. 16 we present the Y_l^0 moments of the $K\pi$ system (the $m \neq 0$ moments are all consistent with zero) for $l \leq 8$. The moments are calculated in the Gottfried-Jackson frame for all events with $-t' < 0.2$ (GeV/c)² and the even moments are also determined for events which are produced backward in that system ($\cos\theta_J < 0$). All of the full moments rise at high $K\pi$ mass due to the effects of the $p\pi^-$ low-mass enhancement. The even moments calculated in the backward hemisphere are free of the diffractive enhancement.

In the $K^*(1420)$ region we observe rises in $\langle Y_4^0 \rangle$ in both the total and backward hemisphere moments. Owing to the complications of the low-mass $p\pi^-$ enhancement, only the backward hemisphere moments show the proper resonant behavior. In the $K^*(1760)$ region the Y_6^0 moment shows a similar behavior. As before, only the backward hemisphere Y_6^0 moment has a resonant shape (but see also the unnormalized full moment in Fig. 3). We interpret this behavior as four-standard deviation evidence that the spin and parity of the $K^*(1760)$ is $J^P = 3^-$. This result is confirmed by the recent

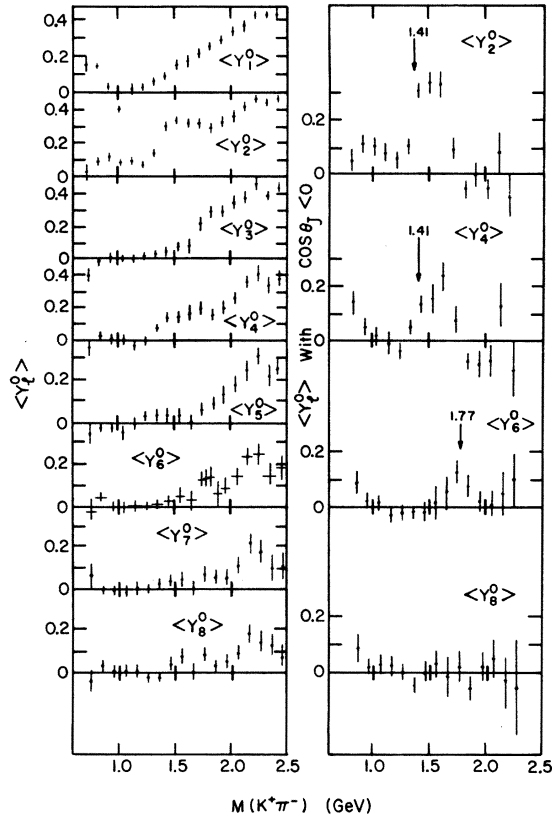


FIG. 16. The Y_l^0 moments of the $K\pi$ system (Jackson frame) for events of reaction (1) with $-t' < 0.2$ (GeV/c)² and $l \leq 8$. The plots on the right-hand side are the even l for events with $\cos \theta_J < 0.0$.

experiment of Baldi *et al.*¹⁶ A maximum-likelihood fit for the diagonal density matrix elements yields $\rho_{00} = 0.75 \pm 0.12$, $\rho_{11} = 0.10 \pm 0.06$, $\rho_{22} = 0.10 \pm 0.08$, and $\rho_{33} = 0.06 \pm 0.06$. The large value of ρ_{00} indicates that pion exchange plays a dominant role in the production process.

The spin and parity of the $K^*(2100)$ cannot be determined solely in the backward hemisphere as

there is insufficient data (Fig. 16). Some unnormalized even moments are shown in Fig. 3 as function of $M(K\pi)$ for $-t' < 0.2$ (GeV/c)². In the $K^*(2100)$ region the Y_6^0 and Y_8^0 moments show resonant behavior whereas the Y_{10}^0 moment remains consistent with zero. The statistical significance of the effect is about three standard deviations and thus $J^P = 4^+$ is the preferred spin-parity assignment for the $K^*(2100)$. Since there is interference between the $K^*(2100)$ and the low-mass $\rho\pi^-$ enhancement this spin parity should be checked at another energy. At 12.7 GeV/c Firestone *et al.*¹⁷ have also studied the reaction $K^+n \rightarrow K^+\pi^-p$ and they found a single broad (~ 500 -MeV) high-mass $K\pi$ structure centered at 1.85 GeV. The high-mass portion of their enhancement is also produced primarily for $\cos \theta_J > 0.7$. In the analogous reaction¹² $K^+p \rightarrow K^+\pi^+n$ at 7.3 GeV/c only the $K^*(1760)$ is seen in the $M(K^-\pi^+)$ effective mass plot, but if the events which can interfere with the baryon-dissociation events are selected Eisner¹⁸ has shown that there is evidence for a second peak near 2.06 GeV.

VI. CONCLUSIONS

Evidence for two high-mass K^* states is found. The $K^*(1760)$ has a mass of 1.769 ± 12 MeV and a width of 132 ± 50 MeV. It decays into $K\pi$, $K^*\pi$, $K\rho$, $K^*\rho$, and probably $K\omega$ and $K^*\omega$ and has spin-parity $J^P = 3^-$. The $K^*(2100)$ has a mass of 2115 ± 46 MeV and a width of 300 ± 200 MeV. It decays into $K\pi$, $K^*\pi$, $K\rho$, $K^*\rho$, $K^*(1420)\pi$, and possibly Kf and a 4^+ spin-parity assignment is strongly favored.

ACKNOWLEDGMENTS

We wish to thank the staff of the AGS and 80-in. bubble chamber as well as our scanners, measurers, and technical support staff. We also thank Dr. D. Cords, Dr. R. F. Holland, and Professor F. J. Loeffler, who participated in the early stages of this work.

†Work supported in part by the U. S. Energy Research and Development Administration.

‡Now at Johns Hopkins Research Laboratories, Baltimore, Maryland.

¹D. D. Carmony, D. Cords, H. W. Clopp, A. F. Garfinkel, R. F. Holland, F. J. Loeffler, H. B. Mathis, L. K. Rangan, J. Erwin, R. L. Lander, D. E. Pellett, P. M. Yager, F. T. Meiere, and W. L. Yen, Phys. Rev. Lett. **27**, 1160 (1971).

²D. D. Carmony, in *Particles and Fields-1973*, proceedings of the Berkeley Meeting of the Division of Particles and Fields of the APS, edited by H. H. Bingham, M. Davier, and G. R. Lynch (AIP, New York, 1973), p. 156.

³The number of events given are the data samples used after confidence level and momentum transfer cuts (see text). The cross sections are the total channel cross section including Glauber corrections.

⁴For further details see H. W. Clopp, Jr., Purdue Univ., Ph.D. thesis, 1972 (unpublished).

⁵W. L. Yen, F. T. Meiere, D. D. Carmony, D. Cords, A. F. Garfinkel, F. J. Loeffler, R. L. McIlwain, L. K. Rangan, R. L. Lander, D. E. Pellett, and P. M. Yager, Phys. Rev. D **9**, 1210 (1974).

⁶D. D. Carmony, A. F. Garfinkel, L. K. Rangan, and W. L. Yen, Phys. Rev. D **11**, 3331 (1975).

⁷D. Cords, D. D. Carmony, H. W. Clopp, A. F. Garfinkel, R. F. Holland, F. J. Loeffler, H. B. Mathis, L. K.

- Rangan, J. Erwin, R. L. Lander, D. E. Pellett, P. M. Yager, F. T. Meiere, and W. L. Yen, Phys. Rev. D 4, 1974 (1971).
- ⁸D. Cords, D. D. Carmony, A. F. Garfinkel, F. J. Loeffler, L. K. Rangan, R. L. Lander, D. E. Pellett, P. M. Yager, F. T. Meiere, and W. L. Yen, Nucl. Phys. B54, 109 (1973).
- ⁹The mass cuts are $K^*(890)$: 0.78–1.0 GeV, ρ : 0.64–0.88 GeV, ω : 0.733–0.833 GeV, Δ^* : 1.10–1.32 GeV, and Δ^0 : 1.16–1.30 GeV.
- ¹⁰The scale factor is as used by the Particle Data Group. See Rev. Mod. Phys. 48, S14 (1976).
- ¹¹S. U. Chung, R. L. Eisner, S. D. Protopopescu, N. P. Samios, and R. C. Strand, Phys. Lett. B51, 413 (1974).
- ¹²M. Aguilar-Benitez, S. U. Chung, R. L. Eisner, S. D. Protopopescu, N. P. Samios, and R. C. Strand, Phys. Rev. Lett. 30, 672 (1973).
- ¹³M. Spiro, R. Barloutaud, A. Borg, D. Denegri, C. Wohl, K. Paler, C. Comber, S. N. Tovey, T. P. Shah, B. Chaurand, B. Drevillon, J. N. Gago, and R. A. Salmeron, Phys. Lett. 60B, 389 (1976).
- ¹⁴D. Lissauer, G. Alexander, A. Firestone, and G. Goldhaber, Nucl. Phys. B18, 491 (1970).
- ¹⁵Y. Cho, M. Derrick, D. Johnson, B. Musgrave, T. Wangler, J. Wong, R. Ammar, R. Davis, W. Kroppac, H. Yarger, and B. Werner, Phys. Rev. D 3, 1561 (1971); P. Antich, A. Callahan, R. Carson, C.-Y. Chien, B. Cox, D. Denegri, L. Ettliger, D. Feiock, G. Goodman, J. Hayes, R. Mercier, A. Pevsner, L. Resvanis, R. Sekulin, V. Sreedhar, and R. Zdanis, Nucl. Phys. B29, 305 (1971).
- ¹⁶R. Baldi, T. Boehringer, P. A. Dorsaz, V. Hungerbühler, M. N. Kienzle-Focacci, M. Martin, A. Mermoud, C. Nef, and P. Siegrist, Phys. Lett. 63B, 344 (1976).
- ¹⁷A. Firestone, G. Goldhaber, D. Lissauer, and G. H. Trilling, Phys. Lett. 36B, 513 (1971).
- ¹⁸R. L. Eisner, in Proceedings of the 2nd International Winter Meeting on Fundamental Physics, Formigal, Spain, 1974, p. 79 (unpublished).